

# A Measurement Protocol for the Topological Uhlmann Phase

O. Viyuela<sup>1</sup>, A. Rivas<sup>1</sup>, S. Gasparinetti<sup>2</sup>, A. Wallraff<sup>2</sup>, S. Filipp<sup>3</sup> and M.A. Martin-Delgado<sup>1</sup>

1. *Departamento de Física Teórica I, Universidad Complutense, 28040 Madrid, Spain*

2. *Department of Physics, ETH Zurich, CH-8093 Zurich, Switzerland*

3. *IBM Research - Zurich, 8803 Rüschlikon, Switzerland*

Topological insulators and superconductors at finite temperature can be characterised by the topological Uhlmann phase. However, the direct experimental measurement in condensed matter systems has remained elusive. We explicitly demonstrate that the topological Uhlmann phase can be measured with the help of ancilla states in systems of entangled qubits that simulate a topological insulator. We propose a novel state-independent measurement protocol which does not involve prior knowledge of the system state. With this construction, otherwise unobservable phases carrying topological information about the system become accessible. This enables the measurement of a complete phase diagram including environmental effects. We explicitly consider a realization of our scheme using a circuit of superconducting qubits. This measurement scheme is extendible to interacting particles and topological models with a large number of bands.

PACS numbers: 42.50.Dv, 85.25.-j, 03.65.Vf

**1. Introduction.**— The search for topological phases in condensed matter [1–6] has triggered an experimental race to detect and measure topological phenomena in a wide variety of quantum simulation experiments [7–12]. In quantum simulators the phase of the wave function can be accessed directly, opening a whole new way to measure topological properties [7, 9, 13] beyond the realm of traditional condensed matter. These quantum phases are very fragile, but when controlled and mastered, they can produce very powerful computational systems like a quantum computer [14, 15]. The Berry phase [16] is a special instance of quantum phase, one that is purely geometrical [17] and independent of dynamical effects during the time evolution of a quantum system. When it is invariant under deformations of the path traced out by the system during its evolution, it becomes topological. Topological Berry phases have also acquired a great relevance in condensed matter systems. The now very active field of topological insulators (TIs) and superconductors (TSCs) [1] ultimately owes its topological character to Berry phases [18] associated to the special band structure of these exotic materials.

However, when a TI or a TSC is open to an environment that can cause external noise like thermal fluctuations, these quantum phases are very fragile [19–28] and may not even be well-defined. These phases of matter are very relevant since they are based on the Berry phase acquired by a pure state. The fragility problem has been successfully solved for one-dimensional systems [30] and extended to two-dimensions later [31–33]. The key concept behind this theoretical characterisation is the notion of *Uhlmann phase* [34–38], a natural extension of the Berry phase for density matrices.

Although the topological Uhlmann phase is gauge invariant and thus in principle observable, a fundamental question remains: how to measure a topological Uhlmann phase in a physical system? In this work we address this

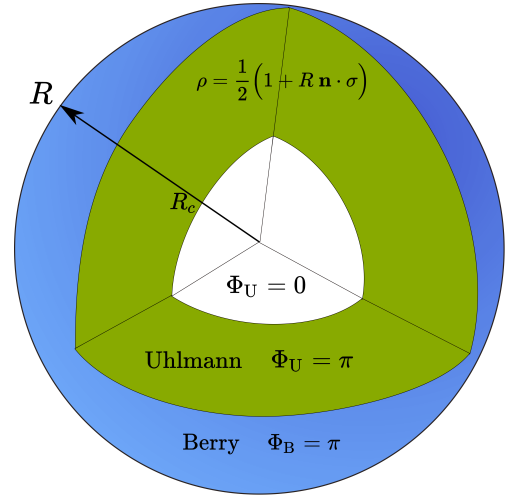


FIG. 1: Topological measures for a single qubit in a mixed state  $\rho = (1-r)|1\rangle\langle 1| + r|0\rangle\langle 0| = \frac{1}{2}(\mathbb{1} + R \mathbf{n} \cdot \boldsymbol{\sigma})$  in the Bloch sphere representation. The mixedness parameter  $r$  between states  $|1\rangle$  and  $|0\rangle$  is encoded into the degree of mixedness  $R = |2r - 1|$ . We compute the Berry  $\Phi_B$  and Uhlmann  $\Phi_U$  phases for non-trivial topological regimes. If  $r \notin \{1, 0\}$  or equivalently  $R < 1$ , then only  $\Phi_U$  is well defined and highlights a non-trivial topological phase ( $\Phi_U = \pi$ ), provided that  $R > R_c = |1 - 2r_{c1,c2}|$ . Here,  $R_c$  denotes the critical amount of noise that the system can withstand while remaining topological.

challenge by: 1) proposing a new protocol to measure experimentally this topological phase, and 2) computing the topological phase diagram for qubits with an arbitrary noise parameter  $r$  [see Eq. (S1)], described by Hamiltonian (3). To this end, we employ an ancillary system as a part of the measurement apparatus, in such a way that by encoding the temperature (or mixedness) of the system in the entanglement with that ancilla, the Uhlmann phase appears as a relative phase that can be

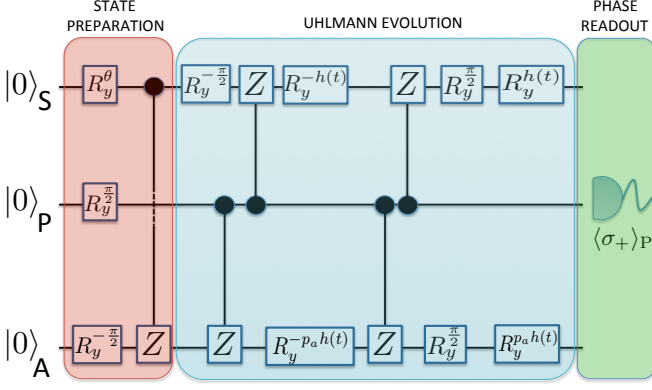


FIG. 2: Circuit diagram to measure the topological Uhlmann phase, e.g., with superconducting circuits as explained in the text. The circuit represents the decomposition of the bi-local unitary evolution  $U_S(t) \otimes U_A(t)$  into elementary single and two-qubit gates [42]. The gate  $R_y^\theta$  represents a single qubit rotation about the y-axis for an angle  $\theta$ , and  $Z$  stands for a controlled-phase gate.

determined by interferometric techniques. The difficulty with this type of measurement is that it requires a high level of control, beyond the reach of condensed matter experiments. On the contrary, this situation is specially well-suited for a quantum simulation scenario realised, for example, with superconducting qubits [39–41]. A summary and a comparison with pure state topological measures are shown in Fig. 1.

This approach leads naturally to construct a state independent protocol that detects whether a given mixed state is topological in the Uhlmann sense (see Fig. 2). Our proposal also provides a novel quantum simulation of the AIII class [43, 44] of topological insulators (those with chiral symmetry) in the presence of disturbing external noise. Other cases of two-dimensional TIs, TSCs and interacting systems can also be achieved by appropriate modifications mentioned in the conclusions.

**2. Topological Uhlmann phase for qubits.**— We briefly present the main ideas of the Uhlmann approach for a qubit that simulates two-band models of TIs and TSCs. Let  $\theta(t)|_{t=0}^1$  define a closed trajectory along a family of single qubit density matrices parametrised by  $\theta$ ,

$$\rho_\theta = (1-r)|1_\theta\rangle\langle 1_\theta| + r|0_\theta\rangle\langle 0_\theta|, \quad (1)$$

where  $r$  stands for the mixedness parameter between the  $\theta$  dependent “ground” state  $|1_\theta\rangle$  and the “excited” state  $|0_\theta\rangle$ , e.g. that of a transmon qubit [45]. Note that  $\rho_\theta$  can be treated as a pure state  $|\Psi_\theta\rangle$  in an enlarged Hilbert space  $\mathcal{H} = \mathcal{H}_S \otimes \mathcal{H}_A$ , where  $S$  stands for system and  $A$  for the ancilla degrees of freedom. A second transmon can be used to realise the ancilla. This process is called purification, and satisfies the constraint  $\rho_\theta = \text{Tr}_A(|\Psi_\theta\rangle\langle\Psi_\theta|)$ , where  $\text{Tr}_A$  takes the partial trace over the ancilla. The set of purifications  $|\Psi_\theta\rangle$  generates the family of density

matrices  $\rho_\theta$ .

The evolution of the purification (system qubit  $S$  and ancilla qubit  $A$ ) can be written as

$$|\Psi_{\theta(t)}\rangle = \sqrt{r}U_S(t)|0\rangle_S \otimes U_A(t)|0\rangle_A + \sqrt{1-r}U_S(t)|1\rangle_S \otimes U_A(t)|1\rangle_A, \quad (2)$$

where  $|0\rangle = \begin{pmatrix} 1 \\ 0 \end{pmatrix}$  and  $|1\rangle = \begin{pmatrix} 0 \\ 1 \end{pmatrix}$  is the standard qubit basis, and  $U_S(t)$  and  $U_A(t)$  are unitary matrices determined by the system Hamiltonian and the Uhlmann parallel transport condition. Namely, parallel transport requires that the distance between two infinitesimally closed purifications  $\| |\Psi_{\theta(t+dt)}\rangle - |\Psi_{\theta(t)}\rangle \|^2$  reaches a minimum value [34]. Physically, this condition ensures that the outcome quantum phase will be purely geometrical and without dynamical contributions. This is actually a source of robustness, since variations on the transport velocity will not change the resulting phase. To form the state in Eq. (S21), entanglement between two superconducting qubits can be created, for instance, via their common coupling to a microwave cavity [46].

Next, we consider the Hamiltonian of a topological insulator in the AIII chiral-unitary class [43, 44]

$$\begin{aligned} H_\theta &= \frac{G_\theta}{2} \mathbf{n}_\theta \cdot \boldsymbol{\sigma}, \\ \mathbf{n}_\theta &= \frac{2}{G_\theta} (\sin \theta, 0, M + \cos \theta), \\ G_\theta &= 2\sqrt{1 + M^2 + 2M \cos \theta}. \end{aligned} \quad (3)$$

where  $G_\theta$  stands for the two-level gap, and  $\mathbf{n}_\theta$  is a unit vector called winding vector [30]. The parameter  $\theta$  can be varied in time, and it will play the role of the crystalline momentum in topological insulators and superconductors [1]. When invoking the rotating wave approximation this model describes, e.g. the dynamics of a driven transmon qubit [11, 13]. The detuning  $\Delta = 2(\cos \theta + M)$  is parametrised in terms of the crystalline momentum  $\theta$  and a hopping amplitude  $M$ , whereas the coupling strength between the qubit and the incident microwave field is given by  $\Omega = 2 \sin \theta$ .

For pure states in those topological materials ( $r \in \{0, 1\}$ ), non-trivial topology can be witnessed by the winding number. This is defined as the angle swept out by  $\mathbf{n}_\theta$  as  $\theta$  varies from 0 to  $2\pi$ , namely,

$$\omega_1 := \frac{1}{2\pi} \oint \left( \frac{\partial_\theta \mathbf{n}_\theta^x}{n_\theta^z} \right) d\theta. \quad (4)$$

Then, using Eq. (3) and Eq. (S29), the system is topological ( $\omega_1 = 1$ ) when the hopping amplitude is less than unity ( $M < 1$ ) and trivial ( $\omega_1 = 0$ ) if  $M > 1$ . In fact, the topological phase diagram coincides with the one given by the Berry phase acquired by the ground state  $|1\rangle_\theta$  (or the excited state  $|0\rangle_\theta$ ) of Hamiltonian (3) when  $\theta$  varies from 0 to  $2\pi$ , (see Sec. III of the SM [47]).

The computation of the evolutions  $U_S$  and  $U_A$  in Eq. (S21) for Hamiltonian (3), yields the following form

$$U_S(t) = e^{-i \int_0^t h(t') dt' \sigma_y}, \quad U_A(t) = e^{-i p_a \int_0^t h(t') dt' \sigma_y}, \quad (5)$$

with  $h(t) := \frac{\partial_t n_t^x}{2n_t^z}$ . The unitary  $U_S$  implements the eigenstate transport  $|1_\theta\rangle = U_S|1\rangle$  and  $|0_\theta\rangle = U_S|0\rangle$ , and  $U_A = (U_S)^{p_a}$  with  $p_a \in [0, 1]$  defined as the ancillary weight. When  $p_a = p_r := 2\sqrt{r(1-r)}$ , the purification precisely follows Uhlmann parallel transport. For more details, see Sec. I and II of the SM [47].

Now, from Eq. (S21) it is possible to define the relative phase  $\Phi_M$  between the initial  $|\Psi_{\theta(0)}\rangle$  and the final state, i.e.  $|\Psi_{\theta(t_f)}\rangle$ . For Hamiltonian (3), density matrix (S1) and purification (S21), we find

$$\begin{aligned} \Phi_M &:= \arg[\langle \Psi_{\theta(0)} | \Psi_{\theta(t_f)} \rangle] = \\ &= \arg[\cos(I_f) \cos(p_a I_f) + p_r \sin(I_f) \sin(p_a I_f)], \end{aligned} \quad (6)$$

where  $I_f := \int_0^{t_f} h(t') dt'$ . In particular, if  $p_a = p_r$ , the relative phase  $\Phi_M$  is called the Uhlmann phase  $\Phi_U$ . This phase is a gauge independent quantity [34], defined through the parallel transport of the purification  $|\Psi_\theta\rangle$ . It also characterises topological order of density matrices [30–33], (see Sec. III of the SM [47]).

For a closed path  $t_f = 1$ , the integral  $I_f = \pi\omega_1 = \Phi_B$  is precisely the topological Berry phase. In that case the Uhlmann phase simplifies to

$$\Phi_U = \arg\{\cos[(1 - 2p_r)\pi\omega_1]\}. \quad (7)$$

From this, we can deduce the topological properties of these topological materials in the presence of external noise, as measured by the parameter  $r$  [Eq. (S1)]. This is depicted in Fig. 1. Namely, if  $M > 1$  then  $\omega_1 = 0$ , and  $\Phi_U = 0$  for every mixedness parameter  $r$ . If  $M < 1$  then  $\omega_1 = 1$  and hence  $\Phi_U = \arg[-\cos(2\pi\sqrt{r(1-r)})]$ . If the state is pure ( $r = 0$ ), then  $\Phi_U^0 = \pi$ , recovering the same topological phase given by the winding number and the Berry phase. However, for  $r \neq 0$  there are critical values of the mixedness  $r_c$  at which  $p_r = 0.5$ , and the Uhlmann phase, according to Eq. (7), jumps from  $\pi$  to zero (see Fig. 1). The first  $r_{c1} = \frac{1}{4}(2 - \sqrt{3})$  signals the mixedness at which the system loses the topological character of the ground state. Moreover, there exists another  $r_{c2} = 1 - r_{c1}$  at which the system becomes topological again due to the topological character of the excited state ( $r \rightarrow 1$ ). Actually,  $p_r(r = r_c) = 0.5$  implies that whenever the state satisfies  $p_r < 0.5$ , the system is topological in the Uhlmann sense, as long as  $M < 1$ . The new reentrance in the topological phase at  $r_{c2}$  was absent in previous works [30–32].

**3. State-independent protocol.**— The application of  $U_S(t)$  and  $U_A(t)$  with  $p_a = p_r$  to the purification  $|\Psi_{\theta(t)}\rangle$  implements the Uhlmann parallel transport and hence  $\Phi_M = \Phi_U$ . However, this would imply knowing the mixedness

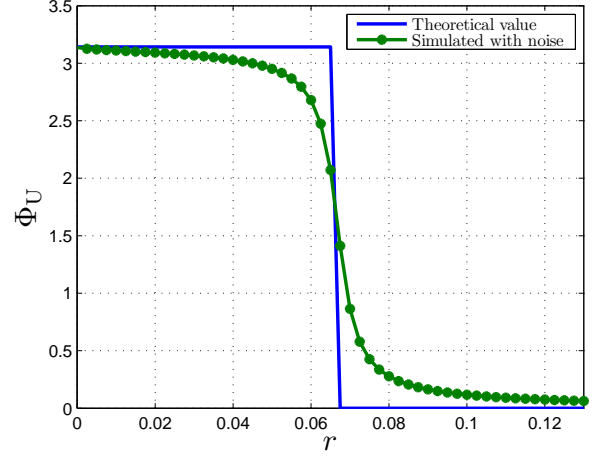


FIG. 3: Comparison between the theoretical value of the Uhlmann phase  $\Phi_U$  and a realistic noise simulation, as a function of the mixedness  $r$ . We have taken into account experimental imperfections such as finite coherence time or residual interactions. The topological transition is clearly appreciable also in the presence of noise. Details can be found in Sec. IV of the SM [47].

parameter  $r$  of the state beforehand, which is not always possible. Hence, we modify the previous protocol to measure the topological Uhlmann phase without prior knowledge of the state  $\rho$  and its mixedness parameter  $r$  in the following way.

Firstly, we assume a linear variation  $\theta(t) = v_s t$ , fix  $v_s = 2\pi$  and consider open holonomies  $\frac{1}{2} < t_f < 1$  covering more than half of the complete path. No previous knowledge of the state is assumed to perform the evolution. Hence, the ancillary weight  $p_a$  might be different than the unknown weight  $p_r$  in Eq. (S21), but still satisfying  $0 \leq p_a \leq 1$ . From Eq. (S24), the overlap  $\langle \Psi_{\theta=0} | \Psi_{\theta=2\pi t_f} \rangle$  is always real and thus the phase  $\Phi_M$  has to be 0 or  $\pi$ , depending on both the weight  $p_r$  associated to the state  $\rho_\theta$  [Eq. (S1)] and the ancillary weight  $p_a$ .

There is an intuitive reason why we can get topological information out of a phase that is associated to a path that covers more than half of the non-trivial topological loop. Indeed,  $h(t)$  is symmetric around  $t = \frac{1}{2}$ . Then, once we have covered half of the path, we know about the topology of the whole system thanks to this symmetry. Therefore, even an open path for  $\frac{1}{2} < t_f < 1$  can be considered global.

Using Eq. (S24), we compute the value of  $p_a^c$  (where the superindex  $c$  stands for critical) at which  $\Phi_M$  goes abruptly from  $\pi$  to 0 as a function of  $p_r$  and  $I_f$ ,

$$p_a^c = \frac{-1}{I_f} \arctan\left(\frac{1}{p_r \tan(I_f)}\right), \quad (8)$$

which is a monotonically decreasing function of  $p_r$ .

At this point, we are in position to deduce the topological

properties for the open quantum system without a priori knowledge of its density matrix:

(a) For the trivial case  $M > 1$ , there is no critical value  $p_a^c$  since  $\Phi_M = 0$  – equivalent to the Uhlmann phase  $\Phi_U$  – for every  $p_r$  and  $p_a$ .

(b) For the case  $M < 1$  and  $\frac{1}{2} < t_f < 1$ , we compute the critical weight  $p_T := p_a^c(p_r = 0.5)$  at which  $\Phi_M$  goes to zero at the topological frontier  $p_r = 0.5$ . A given state is topological if  $p_r < 0.5$ , and not topological if  $p_r > 0.5$ . Therefore, applying the gates  $U_S$  and  $U_A$  with  $p_a = p_T$  may give either

- i)  $\Phi_M(p_T) = 0$  implying  $p_a^c < p_T$  and hence  $p_r > 0.5$ , as  $p_a^c$  always decreases with  $p_r$ . Thus, the system is in a trivial phase.
- ii)  $\Phi_M(p_T) = \pi$  implying  $p_a^c > p_T$ , thus  $p_r < 0.5$ . The system is in a non-trivial topological phase.

Therefore we have been able to map the phase  $\Phi_M(p_T)$  to the topological Uhlmann phase  $\Phi_U$ . A more detailed explanation is given in Sec. III of the SM [47].

Finally, in order to experimentally measure the Uhlmann phase, we need to include an extra third qubit acting as a probe  $P$ . The measurement protocol is described in Fig. 2:

**Step 1.** Following Eq. (S24), we prepare the initial state  $|\Psi_{\theta=0}\rangle \otimes |0\rangle_P$  (red block of Fig. 2) using single qubit rotations  $R_y^\theta$  about the y-axis for an angle  $\theta$  and a two-qubit entangling gate, e.g. a controlled phase gate for frequency-tunable transmons [48].

**Step 2.** We apply the bi-local unitary  $U_S(t) \otimes U_A(t)$  on  $S \otimes A$  conditional to the state of the probe  $P$ . This is accomplished by single qubit rotations about an angle determined by  $h(t)$  and  $p_a$  (blue block of Fig. 2), and two-qubit controlled-phase gates. As a consequence the 3 qubits  $\{S, A, P\}$  are in the superposition

$$|\Phi\rangle_{SAP} = \frac{1}{\sqrt{2}}(|\Psi_{\theta=0}\rangle \otimes |0\rangle_P + |\Psi_{\theta=2\pi t_f}\rangle \otimes |1\rangle_P). \quad (9)$$

**Step 3.** After the holonomic evolution has been completed, we read out  $\Phi_M$  from the state of the probe qubit. Tracing out the system and ancilla in Eq. (9), the reduced state for the probe qubit is

$$\rho_P = \frac{1}{2} \left( \mathbb{1} + \text{Re}(\langle \Psi_{\theta=0} | \Psi_{\theta=2\pi} \rangle) \sigma_x + \text{Im}(\langle \Psi_{\theta=0} | \Psi_{\theta=2\pi} \rangle) \sigma_y \right). \quad (10)$$

Thus, by measuring the expectation values  $\langle \sigma_x \rangle$  and  $\langle \sigma_y \rangle$  (green block of Fig. 2), we can retrieve  $\Phi_M$  in the form of

$$\begin{aligned} \Phi_M &= \arg[\langle \sigma_x \rangle + i \langle \sigma_y \rangle] = \\ &= \arg[\langle \Psi_{\theta=0} | U_S(t_f) \otimes U_A(t_f) | \Psi_{\theta=0} \rangle], \end{aligned} \quad (11)$$

Complementary, if we set  $p_a = p_r$  we are also able to test the Uhlmann parallel transport condition by measuring  $\Phi_M$  at each step along the holonomy.

Under realistic experimental conditions, decoherence and dissipation will adversely affect the measured topological Uhlmann phase. We have thus included a realistic noise simulation based on modest assumptions on the coherence of three transmon qubits. With typical gate durations of 25 and 45 ns for single and two-qubit gates, relaxation times of  $T_1 \approx 5\mu\text{s}$  and coherence times of  $T_2 \approx 3\mu\text{s}$  [49], we clearly observe a phase jump of  $\pi$  for the Uhlmann phase as shown in Fig. 3. More details about the simulation are given in the supplementary material [47].

**5. Conclusions and Outlook.**— We have devised an explicit protocol to perform a realistic measurement of the Uhlmann phase in topological insulators and superconductors implementable in a minimal quantum simulator with 3 superconducting qubits. In particular, we exploit the quantum simulator to realize a controlled coupling of the system to an environment represented by the ancilla degree of freedom. The proposed state-independent protocol allows us to classify states of topological systems according to the Uhlmann measure. Interestingly, some thermodynamical connections to the topological Uhlmann phase have been recently addressed [50].

An increase of experimental resources such as the number of qubits, the speed and fidelity of the quantum gates, etc. would allow us to study novel topological phenomena with superconducting qubits. In particular, by including interactions in the model Hamiltonian we could test different new features: quantum simulations of thermal topological transitions in 2D TIs and TSCs, the interplay between noise and interactions inside a topological phase, etc. These new effects could be achieved since a system with more interacting qubits can be mapped onto models for interacting fermions with spin [12]. Further details can be found in Sec. V of the SM [47]. Although such a proposal would be experimentally more demanding, it represents a clear outlook when the controllability of more qubits and the possibility of performing more gates with high fidelity would be at hand.

M.A.MD., A.R. and O.V. thank the Spanish MINECO grant FIS2012-33152, the CAM research consortium QUITEMAD+ S2013/ICE-2801, the U.S. Army Research Office through grant W911NF-14-1-0103, FPU MEC Grant and Residencia de Estudiantes. S.G., A.W. and S.F. acknowledge support by the Swiss National Science Foundation (SNF, Project 150046).

- 
- [1] M. Z. Hasan and C. L. Kane, Rev. Mod. Phys. **82**, 3045 (2010); X.-L. Qi and S.-C. Zhang, Rev. Mod. Phys. **83**, 1057 (2011); B. A. Bernevig and T. L. Hughes, *Topological Insulators and Topological Superconductors* (Princeton University Press, New Jersey, 2013); and references therein
  - [2] B. A. Bernevig, T. L. Hughes, S.-C. Zhang, Science **314**, 5806 1757-1761 (2006).

- [3] M. Koenig et al. Science **318**, 5851 766-770 (2007).
- [4] T. H. Hsieh, H. Lin, J. Liu, W. Duan, A. Bansil and L. Fu, Nature Communications **3**, 982 (2012).
- [5] P. Dziawa et al. Nature Materials **11**, 1023-1027 (2012).
- [6] S. Xu et al. Science **349**, 6248 613-617 (2015).
- [7] M. Atala, M. Aidelsburger, J. T. Barreiro, D. Abanin, T. Kitagawa, E. Demler and I. Bloch, Nat. Phys. **9**, 795 (2013).
- [8] G. Jotzu, M. Messer, R. Desbuquois, M. Lebrat, T. Uehlinger, D. Greif, T. Esslinger, Nature **515**, 237-240 (2014)
- [9] L. Duca, T. Li, M. Reitter, I. Bloch, M. Schleier-Smith, U. Schneider, Science **347**, 288 (2015).
- [10] T. Li, L. Duca, M. Reitter, F. Grusdt, E. Demler, M. Endres, M. Schleier-Smith, I. Bloch, U. Schneider, Science **352**, 1094 (2016).
- [11] M. D. Schroer et al. Phys. Rev. Lett. **113**, 050402 (2014).
- [12] P. Roushan et al. Nature **515**, 241-244 (2014).
- [13] P. J. Leek et al. Science **318** 5858 1889-1892 (2007).
- [14] M. A. Nielsen and I. L. Chuang, *Quantum Computation and Quantum Information* (Cambridge University Press, Cambridge, 2000).
- [15] A. Galindo and M.A. Martin-Delgado, Rev. Mod. Phys. **74** 347-423, (2002).
- [16] M. V. Berry, Proc. R. Soc. A **392**, 45 (1984).
- [17] A. Shapere and F. Wilczek, *Geometric Phases in Physics* (World Scientific, Singapore, 1989).
- [18] J. Zak, Phys. Rev. Lett. **62**, 2747 (1989).
- [19] O. Viyuela, A. Rivas and M. A. Martin-Delgado, Phys. Rev. B **86**, 155140 (2012).
- [20] A. Rivas, O. Viyuela and M. A. Martin-Delgado, Phys. Rev. B **88**, 155141 (2013).
- [21] L. Mazza, M. Rizzi, M. D. Lukin and J. I. Cirac, Phys. Rev. B **88**, 205142 (2013).
- [22] C.-E. Bardyn, M. A. Baranov, C. V. Kraus, E. Rico, A. Imamoglu, P. Zoller, S. Diehl, New J. Phys. **15** (2013).
- [23] E. P. L. van Nieuwenburg and S. D. Huber, Phys. Rev. B **90**, 075141 (2014).
- [24] H. Z. Shen, W. Wang, X. X. Yi, Scientific Reports **4**, 6455 (2014).
- [25] H. Dehghani, T. Oka, and A. Mitra, Phys. Rev. B **90**, 195429 (2014).
- [26] Y. Hu, Z. Cai, M. Baranov, and P. Zoller, Phys. Rev. B **92**, 165118 (2015).
- [27] D. Linzner, F. Grusdt, M. Fleischhauer, arXiv: 1605.00756 (2016).
- [28] P. W. Claeys, S. De Baerdemacker, and D. Van Neck, Phys. Rev. B **93**, 220503(R) (2016).
- [29] F. Lemini, D. Rossini, R. Fazio, S. Diehl, and L. Mazza, Phys. Rev. B **93**, 115113 (2016).
- [30] O. Viyuela, A. Rivas and M. A. Martin-Delgado, Phys. Rev. Lett **112**, 130401 (2014).
- [31] O. Viyuela, A. Rivas and M. A. Martin-Delgado, Phys. Rev. Lett **113**, 076408 (2014).
- [32] Z. Huang and D. P. Arovas, Phys. Rev. Lett. **113**, 076407 (2014).
- [33] O. Viyuela, A. Rivas and M. A. Martin-Delgado, 2D Mater. **2** 034006 (2015).
- [34] A. Uhlmann, Rep. Math. Phys. **24**, 229 (1986).
- [35] E. Sjöqvist, A. K. Pati, A. Ekert, J. S. Anandan, M. Ericsson, D. K. L. Oi and V. Vedral, Phys. Rev. Lett. **85**, 2845 (2000).
- [36] M. Ericsson, A. K. Pati, E. Sjöqvist, J. Brännlund and D. K. L. Oi, Phys. Rev. Lett. **91**, 090405 (2003).
- [37] J. Åberg, D. Kult, E. Sjöqvist, and D. K. L. Oi, Phys. Rev. A **75**, 032106 (2007).
- [38] J. Zhu, M. Shi, V. Vedral, X. Peng, D. Suter and J. Du, EPL **94** 20007 (2011).
- [39] R. J. Schoelkopf and S. M. Girvin, Nature, **451**, 664-669 (2008).
- [40] R. Barends *et al*, Nature communications, **6**, 7654 (2015).
- [41] Y. Salathé, M. Mondal, M. Oppliger, J. Heinsoo, P. Kurpiers, A. Potocnik, A. Mezzacapo, U. Las Heras, L. Lamata, E. Solano, S. Filipp, and A. Wallraff, Phys. Rev. X, **5**, 021027 (2015).
- [42] A. Galindo and M.A. Martin-Delgado, Rev. Mod. Phys. **74** 347-423, (2002).
- [43] A. P. Schnyder, S. Ryu, A. Furusaki and A. W. W. Ludwig, Phys. Rev. B **78**, 195125 (2008).
- [44] A. Kitaev, AIP Conf. Proc. **1134**, 22 (2009).
- [45] J. Koch, T. M. Yu, J. Gambetta, A. A. Houck, D. I. Schuster, J. Majer, A. Blais, M. H. Devoret, S. M. Girvin, and R. J. Schoelkopf, Phys. Rev. A **76**, 042319 (2007).
- [46] A. Blais, J. Gambetta, A. Wallraff, D. I. Schuster, S. M. Girvin, M. H. Devoret, and R. J. Schoelkopf, Phys. Rev. A **75**, 032329 (2007).
- [47] Supplementary Material.
- [48] F. W. Strauch, P. R. Johnson, A. J. Dragt, C. J. Lobb, J. R. Anderson, and F. C. Wellstood, Phys. Rev. Lett. **91**, 167005 (2003).
- [49] L. Steffen *et al*. Nature, **500**, 319 (2013).
- [50] S.N. Kempkes, A. Quelle, C. Morais Smith, arXiv: 1607.03373 (2016).

## SUPPLEMENTARY MATERIAL

### I. Uhlmann phase for qubit systems

The Uhlmann phase extends the notion of the geometric Berry phase from pure quantum states (Berry) to mixed quantum states described by density matrices. Uhlmann was first to study this problem from a rigorous mathematical perspective [1] and to find a satisfactory solution [2–5].

Let  $\theta(t)|_{t=0}^1$  define a trajectory along a family of single qubit density matrices parametrised by  $\theta$ ,

$$\rho_\theta = (1-r)|1_\theta\rangle\langle 1_\theta| + r|0_\theta\rangle\langle 0_\theta|, \quad (\text{S1})$$

where  $r$  stands for the degree of mixedness between the ground state  $|1_\theta\rangle$  and the excited state  $|0_\theta\rangle$ . Note that  $\rho_\theta$  can always be viewed as a pure state  $|\Psi_\theta\rangle$  in an enlarged Hilbert space  $\mathcal{H} = \mathcal{H}_S \otimes \mathcal{H}_A$ , where  $S$  stands for system and  $A$  for the ancilla degrees of freedom. This process is called purification, and satisfies the constraint  $\rho_\theta = \text{Tr}_A(|\Psi_\theta\rangle\langle\Psi_\theta|)$ . The set of purifications  $|\Psi_\theta\rangle$  generates the family of density matrices  $\rho_\theta$ . This aims to be the density-matrix analog to the standard situation where vector states  $|\psi\rangle$  span a Hilbert space and generate pure states by the relation  $\rho = |\psi\rangle\langle\psi|$ . Actually, the phase freedom of pure states,  $U(1)$ -gauge freedom, is generalised to a  $U(n)$ -gauge freedom ( $n$  is the dimension of the density matrix). This occurs since  $|\Psi_\theta\rangle$  and  $V_A^t|\Psi_\theta\rangle$  are purifications of the same density matrix for some unitary operator  $V_A^t$  acting on the ancilla degrees of freedom. The superindex  $t$  denotes the transposition with respect to the standard qubit basis. If the trajectory defined by  $\theta(t)$  is closed  $\rho_{\theta(1)} = \rho_{\theta(0)}$ , the initial and final purifications must differ just in some unitary transformation  $V_A^t$ ,  $|\Psi_{\theta(1)}\rangle = V_A^t|\Psi_{\theta(0)}\rangle$ . Hence, by analogy to the pure state case, Uhlmann defines a parallel transport condition such that  $V_A$  is constructed by imposing that the distance between two infinitesimally closed purifications,  $\|\Psi_{\theta(t+dt)}\rangle - |\Psi_{\theta(t)}\rangle\|^2$ , reaches its minimum value. Then it is possible to write

$$V_A = \mathcal{P}e^{\int A_U}, \quad (\text{S2})$$

where  $\mathcal{P}$  stands for the path ordering operator along the trajectory  $\theta(t)|_{t=0}^1$ , and  $A_U$  is the so-called Uhlmann connection form [1, 6, 7].

The Uhlmann geometric phase is defined from the mismatch between the initial point  $|\Psi_{\theta(0)}\rangle$  and the final point after the parallel transportation, i.e.  $|\Psi_{\theta(1)}\rangle$ ,

$$\Phi_U := \arg[\langle\Psi_{\theta=0}|\Psi_{\theta=1}\rangle] = \arg\text{Tr}[\rho_{\theta(0)}V_A] \quad (\text{S3})$$

This phase is a gauge independent quantity [1–3], that comes from the parallel transport of the purification  $|\Psi_\theta\rangle$ .

The most explicit formula for the Uhlmann connection was given by Hübner [4],

$$A_U = \sum_{\theta,i,j} |\psi_\theta^i\rangle \frac{\langle\psi_\theta^i|[(\partial_\theta\sqrt{\rho_\theta}), \sqrt{\rho_\theta}]|\psi_\theta^j\rangle}{p_\theta^i + p_\theta^j} \langle\psi_\theta^j|d\theta, \quad (\text{S4})$$

in the spectral basis of  $\rho_\theta = \sum_j p_\theta^j |\psi_\theta^j\rangle\langle\psi_\theta^j|$ . The parameter  $\theta$  may play the role of the crystalline momentum in condensed matter systems.

The derivative of the square-root of the density matrix with respect to the transport parameter  $\theta$  is given by

$$\begin{aligned} \partial_\theta\sqrt{\rho_\theta} &= \sqrt{(1-r)}(|\partial_\theta 1_\theta\rangle\langle 1_\theta| + |1_\theta\rangle\langle\partial_\theta 1_\theta|) + \\ &+ \sqrt{r}(|\partial_\theta 0_\theta\rangle\langle 0_\theta| + |0_\theta\rangle\langle\partial_\theta 0_\theta|). \end{aligned} \quad (\text{S5})$$

We can simplify the connection  $A_U$  in (S4), for density matrix (S1) and Hamiltonian (3) in the main text. We substitute Eq. (S5) in Eq. (S4), and take into account that the summation indices in Eq. (S4) only runs over the states  $|1_\theta\rangle$  and  $|0_\theta\rangle$ , obtaining

$$\begin{aligned} A_U &= \left[ (1-p_r)\langle 1|\partial_\theta 0_\theta\rangle |0_\theta\rangle\langle 1_\theta| \right. \\ &\quad \left. + (1-p_r)\langle 0_\theta|\partial_\theta 1_\theta\rangle |0_\theta\rangle\langle 1_\theta| \right] d\theta, \end{aligned} \quad (\text{S6})$$

where  $p_r = 2\sqrt{r(1-r)}$ .

For computational purposes, we fix the gauge for the eigenstates of the system Hamiltonian [Eq. (3) of the main text] such that,

$$|0_\theta\rangle = \frac{1}{\sqrt{1+g^2(\theta, M)}} \begin{pmatrix} 1 \\ g(\theta, M) \end{pmatrix}, \quad (\text{S7})$$

$$|1_\theta\rangle = \frac{1}{\sqrt{1+g^2(\theta, M)}} \begin{pmatrix} g(\theta, M) \\ -1 \end{pmatrix}, \quad (\text{S8})$$

where

$$g(\theta, M) := \frac{\sin\theta}{M + \cos\theta + \sqrt{1+M^2+2M\cos\theta}}. \quad (\text{S9})$$

From Eq. (S7) and Eq. (S8), we compute

$$\begin{aligned} \langle 0_\theta|\partial_\theta 1_\theta\rangle &= \frac{\partial_\theta n_\theta^x}{2n_\theta^z} = \frac{1+M\cos\theta}{2+2M^2+4M\cos\theta}, \\ |0_\theta\rangle\langle 1_\theta| - |1_\theta\rangle\langle 0_\theta| &= \begin{pmatrix} 0 & -1 \\ 1 & 0 \end{pmatrix}, \end{aligned} \quad (\text{S10})$$

where  $n_\theta^i$  is the  $i$ -th component of the winding vector. Finally, we insert Eqs. (S10) in Eq. (S6) and obtain

$$A_U = -i(1-p_r)\frac{\partial_\theta n_\theta^x}{2n_\theta^z}\sigma_y d\theta. \quad (\text{S11})$$

As the connection in Eq. (S11) commutes for different values of  $\theta$ , we can drop the path ordering that appears

in the expression for the Uhlmann unitary [Eq. (S2)], and get the simplified equation

$$V_A(\theta) = e^{-i(1-p_r) \int_0^\theta \frac{\partial_{\theta'} n_{\theta'}^x}{2n_{\theta'}^z} \sigma_y d\theta'}. \quad (\text{S12})$$

Lastly, we substitute Eq. (S12) and Eq. (S1) in Eq. (S3) to compute the Uhlmann phase

$$\Phi_U = \arg \left\{ \cos \left[ \frac{1-2p_r}{2} \int_0^\theta \left( \frac{\partial_{\theta'} n_{\theta'}^x}{n_{\theta'}^z} \right) d\theta' \right] \right\}. \quad (\text{S13})$$

## II. Holonomic time evolution

At this stage, we would like to physically implement the holonomy that has been mathematically described in the previous section. For that purpose, we express the parallel transport generated by parameter  $\theta$ , as a unitary time evolution over system and ancilla  $U_S \otimes U_A$  where the control-parameter is varied in time  $\theta(t)$ . The system unitary evolution  $U_S$  is defined through the relations

$$|0\rangle_{\theta(t)} := U_S(t)|0\rangle, \quad |1\rangle_{\theta(t)} := U_S(t)|1\rangle, \quad (\text{S14})$$

where  $|0\rangle = \begin{pmatrix} 1 \\ 0 \end{pmatrix}$  and  $|1\rangle = \begin{pmatrix} 0 \\ 1 \end{pmatrix}$  is the standard qubit basis. Using the eigenstate equations (S7) and (S8),  $U_S(\theta)$  is obtained straightforwardly,

$$U_S(t) = \frac{1}{\sqrt{1+g^2[\theta(t), M]}} \begin{pmatrix} 1 & -g[\theta(t), M] \\ g[\theta(t), M] & 1 \end{pmatrix}, \quad (\text{S15})$$

where  $g(\theta, M)$  was defined in Eq. (S9).

At this point Eq. (S15) can be expressed as the exponential of a Hamiltonian using the following relations

$$U_S(t) = e^{-i \int_0^t h(t') dt'}, \quad (\text{S16})$$

$$h(t) = i \left( \frac{d\theta}{dt} \right) [\partial_\theta U_S(\theta)] U_S^\dagger(\theta). \quad (\text{S17})$$

We substitute Eq. (S15) into Eq. (S17), arriving at

$$h(t) = \left( \frac{d\theta}{dt} \right) \frac{\partial_{\theta(t)} n_{\theta(t)}^x}{2n_{\theta(t)}^z} \sigma_y, \quad (\text{S18})$$

where we have used Eq. (S10) as well.

The unitary for the ancilla qubit  $U_A$  is determined by combining: 1) the transport of the eigenstates  $|0(1)_\theta\rangle$  through  $U_S(t)$  and 2) the Uhlmann correction  $V_A[\theta(t)]$ , for the purification as a whole to be parallely transported [Eq. (S12)]; hence,

$$U_A(t) = [U_S^\dagger(t) V_U(t)]^t. \quad (\text{S19})$$

Here, the superindex  $t$  denotes the transposition with respect to the standard qubit basis. Further simplifications of Eq. (S19) using Eq. (S18) and Eq. (S12) lead to

$$U_A(t) = e^{-ip_a \int_0^t h(t') dt'}, \quad (\text{S20})$$

with  $p_a = p_r$ .

## III. State-independent phase mapping to the Uhlmann phase

Let us now consider open holonomies [open trajectories given by  $\theta(t)$ ] with the following constraints:

1. We fix a linear ramp  $\theta(t) = v_s t$  and units  $v_s = 2\pi$ .
2. We consider holonomic open paths satisfying  $\frac{1}{2} < t_f < 1$ .
3. Although the Uhlmann parallel transport condition implies  $p_a = p_r$ , let us consider a more general evolution for the ancilla qubit  $p_a \neq p_r$ . The ancilla weight  $p_a$  can be different than  $p_r$ , but still satisfying  $0 \leq p_a \leq 1$ .

The evolution of the purification (system qubit  $S$  and ancilla qubit  $A$ ) can be written as

$$|\Psi_{\theta(t)}\rangle = \sqrt{r} U_S(t) |0\rangle_S \otimes U_A(t) |0\rangle_A + \sqrt{1-r} U_S(t) |1\rangle_S \otimes U_A(t) |1\rangle_A, \quad (\text{S21})$$

where  $U_S(t)$  and  $U_A(t)$  were given in Eq. (S17) and Eq. (S20) respectively.

To shorten the notation, we define  $I_f := \int_0^{t_f} h(t') dt'$  and perform the integration for Hamiltonian (3) in the main text,

$$I_f = \frac{1}{4} \left\{ t_f + 2 \arctan \left[ \frac{(1+M) \cot(t_f/2)}{M-1} \right] + \pi \operatorname{sgn}(1-M) \right\}, \quad \text{if } 0 < t_f < 1. \quad (\text{S22})$$

Now we compute the state  $|\Psi_{\theta(t_f)}\rangle$  at the end of the holonomy

$$\begin{aligned} |\Psi_{\theta(t_f)}\rangle &= \sqrt{r} \left( \cos(I_f) |0\rangle_S - \sin(I_f) |1\rangle_S \right) \otimes \\ &\otimes \left( \cos(p_a I_f) |0\rangle_A - \sin(p_a I_f) |1\rangle_A \right) + \\ &+ \sqrt{1-r} \left( \sin(I_f) |0\rangle_S + \cos(I_f) |1\rangle_S \right) \otimes \\ &\otimes \left( \sin(p_a I_f) |0\rangle_A + \cos(p_a I_f) |1\rangle_A \right) = \\ &= \sqrt{r} \left( \cos(I_f) \cos(p_a I_f) |0\rangle_S \otimes |0\rangle_A + \right. \\ &+ \sin(I_f) \sin(p_a I_f) |1\rangle_S \otimes |1\rangle_A - \\ &- \sin(I_f) \cos(p_a I_f) |1\rangle_S \otimes |0\rangle_A - \\ &- \cos(I_f) \sin(p_a I_f) |0\rangle_S \otimes |1\rangle_A \left. \right) + \\ &+ \sqrt{1-r} \left( \sin(I_f) \sin(p_a I_f) |0\rangle_S \otimes |0\rangle_A + \right. \\ &+ \cos(I_f) \cos(p_a I_f) |1\rangle_S \otimes |1\rangle_A + \\ &+ \cos(I_f) \sin(p_a I_f) |1\rangle_S \otimes |0\rangle_A + \\ &+ \sin(I_f) \cos(p_a I_f) |0\rangle_S \otimes |1\rangle_A \left. \right). \quad (\text{S23}) \end{aligned}$$

We can associate a phase mismatch  $\Phi_M$  between the initial  $|\Psi_{\theta(0)}\rangle$  and the final state, i.e.  $|\Psi_{\theta(t_f)}\rangle$ . This is



given by  $\Phi_M := \arg[\langle \Psi_{\theta=0} | \Psi_{\theta=t_f} \rangle]$ . After a straightforward calculation using Eq. (S23),

$$\Phi_M = \arg \left[ \cos(I_f) \cos(p_a I_f) + p_r \sin(I_f) \sin(p_a I_f) \right]. \quad (\text{S24})$$

This phase generally depends both on the weight associated to the state ( $p_r$ ) and the one applied to the circuit ( $p_a$ ). Moreover, the overlap  $\langle \Psi_{\theta=0} | \Psi_{\theta=t_f} \rangle$  is always real and hence the argument gives  $\Phi_M = 0, \pi$ . In addition, for  $p_a = p_r$  the phase mismatch  $\Phi_M = \Phi_U$ .

Let us now consider an ancillary weight  $p_a \neq p_r$ . From Eq. (S24) we can find the value  $p_a = p_a^c$  (where the superindex  $c$  stands for critical) at which  $\Phi_M$  goes abruptly from  $\pi$  to 0 as a function of  $p_r$  and  $I_f$ ,

$$p_a^c = \frac{-1}{I_f} \arctan \left( \frac{1}{p_r \tan(I_f)} \right). \quad (\text{S25})$$

If we set  $\frac{1}{2} < t_f < 1$ , then  $p_a^c$  is a monotonically decreasing function of  $p_r$ ,

$$\frac{\partial p_a^c}{\partial p_r} = \frac{\tan(I_f)}{I_f [1 + p_r^2 \tan^2(I_f)]} < 0. \quad (\text{S26})$$

If  $M > 1$ , then  $-\pi/2 < I_f < \pi/2$ , which from Eq. (S24) implies that  $\Phi_M = 0$  for any value of  $p_r$  and  $p_a$ . Hence, for the trivial case  $M > 1$ , there is no critical value  $p_a^c$  and  $\Phi_M = 0$  always. This maps  $\Phi_M$  to the Uhlmann phase  $\Phi_U$  at least for this case. On the contrary, if  $M < 1$ , then  $\pi/2 < I_f < \pi$  which implies that  $\tan(I_f) < 0$ . As  $0 < p_r < 1$ , then  $-\arctan\left(\frac{1}{p_r \tan(I_f)}\right) < \pi/2$ . Thus, from Eq. (S24), there is always a solution  $0 < p_a^c < 1$  for any  $p_r$  of the state. As discussed in the main text, the state  $\rho_\theta$  in Eq. (S1) is topological in the Uhlmann sense  $\Phi_U = \pi$ , only if  $M < 1$  and  $p_r < 0.5$ .

Next, we compute the associated critical value of  $p_a$  for the particular case of  $p_r = 0.5$ , defined as

$$p_T := p_a^c(p_r = 0.5) = \frac{-1}{I_f} \arctan \left( \frac{2}{\tan(I_f)} \right). \quad (\text{S27})$$

Note that the true  $p_r$  of the system is unknown as we have assumed no knowledge of the state. But if  $p_r > 0.5$ , then its associated critical value [from Eq. (S25)] is  $p_a^c < p_T$ . This means that applying  $U_A$  with  $p_a = p_T$  and measuring the associated phase  $\Phi_M$  we can extract the following conclusions:

- If we measure  $\Phi_M(p_T) = 0$ , the system is within a trivial phase ( $\Phi_U = 0$ ). Because this implies  $p_a^c < p_T$  and hence  $p_r > 0.5$  ( $\Phi_U = 0$ ), as we have proven that  $p_a^c$  always decreases with  $p_r$ .
- If we measure  $\Phi_M(p_T) = \pi$ , the system is in a topological phase ( $\Phi_U = \pi$ ). Because in that case  $p_a^c > p_T$  and then  $p_r < 0.5$  ( $\Phi_U = \pi$ ).

Hence, we have been able to map  $\Phi_M(p_T)$  to the Uhlmann phase  $\Phi_U$ . However, this mapping only works iff  $\pi/2 < I_f < \pi$  which only occurs for  $M < 1$  and covering more than half of the path  $\frac{1}{2} < t_f < 1$ . Therefore, in order to test if the system is topological or not, we just have to follow the following protocol:

1. We prepare the initial state  $|\Psi_{\theta=0}\rangle \otimes |0\rangle_P$ . The state  $|\Psi_{\theta(t)}\rangle$  is given in Eq. (S21) and  $P$  is an extra probe qubit. This qubit is needed to measure the phase  $\Phi_M$ .
2. We set the length of the evolution  $t_f$  and apply the bi-local unitary  $U_S(t) \otimes U_A(t)$  on  $S \otimes A$  conditional to the state of the probe  $P$ . The ancilla evolution  $U_A(t)$  is carried out taking the ancilla weight  $p_a = p_T$ .
3. After the holonomic evolution has been completed, we read out  $\Phi_M$  from the state of the probe qubit by measuring the argument of the expectation value of  $\langle \sigma_x \rangle_P + i \langle \sigma_y \rangle_P$ .

Finally, we explain why covering at least half of the entire non-trivial path allows us to access topological information, i.e. global. The Hamiltonian of the single-qubit system Eq. (S28) is the circuit QED analog of a topological insulator in the AIII chiral-unitary class,

$$H_\theta = \frac{G_\theta}{2} \mathbf{n}_\theta \cdot \boldsymbol{\sigma}, \quad (\text{S28})$$

where  $G_\theta$  stands for the two-level gap, and  $\mathbf{n}_\theta$  is the winding vector. Both quantities have been defined in Eq. (3) of the main text.

For this model, there is a restriction on the movement of the winding vector  $\mathbf{n}_\theta$  from the sphere  $S^2$  to the circle  $S^1$  on the  $xz$ -plane. Hence, only two of its components  $n_\theta^x$  and  $n_\theta^z$  are different from zero. Therefore, there is a mapping from the family of Hamiltonians  $H_\theta$  on the parameter  $\theta \in S^1$  onto the winding vectors  $\mathbf{n}_\theta \in S^1$ . This mapping  $S^1 \rightarrow S^1$  is characterized by a winding number  $\omega_1$ . This is a topological invariant defined as the angle swept by  $\mathbf{n}_\theta$  when the parameter  $\theta$  is tuned from 0 to  $2\pi$ ,

$$\omega_1 := \frac{1}{2\pi} \oint d\alpha = \frac{1}{2\pi} \oint \left( \frac{\partial_\theta n_\theta^x}{n_\theta^z} \right) d\theta, \quad (\text{S29})$$

where we have used that  $\alpha := \arctan(n_\theta^x/n_\theta^z)$ . For this model, if the parameter  $M < 1$  the system is topological ( $\omega_1 = 1$ ) and if  $M > 1$  the system is in trivial phase ( $\omega_1 = 0$ ). The integral  $I_f$  defined in Eq. (S22) equals the area covered by the winding vector when  $\theta$  is varied. Actually, if the loop is closed ( $t_f = 1$ ), then  $I_f = \pi\omega_1$ . Moreover,  $h(t)$  in Eq. (S18) is symmetric around  $t = \frac{1}{2}$ . So basically when half of the path has been traversed, the information about the whole topology of the system is unveiled. Therefore, an open path that covers more



than half of the non-trivial topological loop ( $\frac{1}{2} < t_f < 1$ ) can be considered global and we can get topological information from the phase  $\Phi_M$ .

#### IV. Noise simulation

We have analyzed the detrimental effect of experimental noise in the proposed measurement scheme. We have modeled this by means of some Liouvillian term  $\mathcal{L}_{\text{noise}}$ , so that the Liouvillian  $\mathcal{L}_0$ , accounting for the idealized dynamics, is in fact substituted by  $\mathcal{L}_0 + \mathcal{L}_{\text{noise}}$ . Specifically, if some gate is performed during a time  $\tau$  via some Hamiltonian  $H_0$ , i.e.  $U_{\text{gate}} = e^{-iH_0\tau}$ , we substitute

$$e^{-iH_0\tau} \rho e^{iH_0\tau} \equiv e^{\mathcal{L}_0\tau} \rho \rightarrow e^{(\mathcal{L}_0 + \mathcal{L}_{\text{noise}})\tau} \rho. \quad (\text{S30})$$

This noise Liouvillian includes typical sources of imperfections: a) some residual ZZ coupling during a C-Phase gate,  $H_{ZZ} = J\sigma_z\sigma_z$ ; b) spontaneous emission and dephasing terms  $\mathcal{L}_-(\rho) = \gamma_-(\sigma_-\rho\sigma_+ - \frac{1}{2}\{\sigma_+\sigma_-, \rho\})$  and  $\mathcal{L}_z(\rho) = \gamma_z(\sigma_z\rho\sigma_z - \rho)$ , respectively.

We have accommodated the values of  $\gamma_-$  and  $\gamma_z$  to the characteristic longitudinal and transverse relaxation times of  $T_1 \sim 5 \mu\text{s}$  and  $T_2 \sim 3 \mu\text{s}$ . The residual ZZ strength has been taken to be about  $J \sim 0.5 \text{ MHz}$  [8]. In addition, we consider  $\tau_{2\pi} \sim 25 \text{ ns}$  and  $\tau_{\text{CP}} \sim 45 \text{ ns}$  as characteristic times for a  $2\pi$ -rotation on a single qubit and the C-Phase gate (see Fig. 2 of the main text), respectively. Waiting times of 5 ns after a single qubit gate and 40 ns after a C-Phase gate are also included.

In Fig. 3 of the main text, we show the result of the simulation including noise in the determination of the topological Uhlmann phase  $\Phi_U$ . We plot the value of the measured Uhlmann phase as a function of the purity of the state  $r$  for  $M < 1$ . Despite the noise, the topological transition is clearly noticed.

#### V. Interacting Systems: New Effects

The protocol to measure the topological Uhlmann phase deals with single-qubit Hamiltonians [Eq. (3) in the main text]. These can be mapped to free-fermion topological insulators. We may identify the ramp parameter  $\theta$  with the crystalline momentum in the Brillouin zone  $k$ .

Nonetheless, more complicated Hamiltonians involving more qubits could be considered in a more general setup. Actually, it has been shown in [9] that an  $L$ -qubit interacting system can be mapped onto two types of systems that will be discussed in what follows.

On the one hand, a system of 2 qubits can be mapped to a system of two interacting fermions with spin  $1/2$ . Therefore, an Uhlmann experiment for interacting 2-qubit Hamiltonians would be the first experimental measurement of a topological phase associated to an interacting system in a mixed state. It would be very interesting to analyse how the interacting term counteracts or enhance the effect that noise produces in the system.

On the other hand, there is a complementary mapping from a many-body interacting spin system to Haldane-like models [10] with  $2^L$  bands. These are free-fermion models but the fact of having more bands opens the possibility of having higher topological quantum numbers. From the point of view of the Uhlmann theory of symmetry-protected topological order at finite temperature, one can clearly envision the possibility of testing topological transitions between non-trivial topological phases solely driven by noise or temperature. This is an effect that only appears in systems with high topological numbers as shown in [11].

- 
- [1] A. Uhlmann, Rep. Math. Phys. **24**, 229 (1986).
  - [2] A. Uhlmann, Ann. Phys. (Leipzig) **46**, 63 (1989).
  - [3] A. Uhlmann, Lett. Math. Phys. **21**, 229 (1991).
  - [4] M. Hübner, Phys. Lett. A **179**, 226 (1993).
  - [5] A. Uhlmann, J. Geom. Phys. **18**, 76 (1996).
  - [6] O. Viyuela, A. Rivas and M. A. Martin-Delgado, Phys. Rev. Lett **112**, 130401 (2014).
  - [7] O. Viyuela, A. Rivas and M. A. Martin-Delgado, 2D Mater. **2** 034006 (2015).
  - [8] L. Steffen *et al.* Nature, **500**, 319 (2013).
  - [9] P. Roushan *et al.* Nature **515**, 241–244 (2014).
  - [10] F. D. M. Haldane, Phys. Rev. Lett. **61**, 2015 (1988).
  - [11] O. Viyuela, A. Rivas and M. A. Martin-Delgado, Phys. Rev. Lett **113**, 076408 (2014).